



## Research Article

# Mechanical behavior of large-diameter pipe elbows under low-cyclic loading

Ercan Şerif KAYA\*

Department of Civil Engineering, Faculty of Engineering, Alanya Alaaddin Keykubat University, 07450, Antalya, Türkiye /  
UCLA (University of California Los Angeles), Department of Civil and Environmental Engineering, USA , 90024, California

## ARTICLE INFO

### Article history

Received: July 20, 2023

Revised: August 17, 2023

Accepted: August 18, 2023

### Keywords:

Pipe elbow, buried pipeline, large-diameter, seismic performance, low-cycle loading

## ABSTRACT

Large-diameter steel pipes are often used for transmitting and distributing water, gas, and oil products from the source to the end user. These pipelines are mainly oriented by using pipe elbows due to their high flexibility along their routes. It is important to understand the mechanical behavior of these critical infrastructure components to promote material sustainability. For this purpose, a rigorous 3D finite element model is employed to investigate the mechanical behavior of large-diameter pipe elbows with varying elbow angles such as 90°, 60°, and 30°. Moreover, geometrical and material nonlinearities capture the pipes' ratcheting behavior even under pressurized and unpressurized scenarios. It is seen that the pipes with a larger elbow angle can endure a higher number of cycles before they reach their limit states. In addition, pipe elbows behave similarly to straight pipes as the elbow angle decreases and becomes more vulnerable to plastic deformations such as kink and buckling under bending loads.

**Cite this article as:** Kaya, EŞ. (2023). Mechanical behavior of large-diameter pipe elbows under low-cyclic loading. *J Sustain Const Mater Technol*, 8(3), 243–250.

## 1. INTRODUCTION

Curved pipes, also often referred to as pipe bends or elbows, are critical infrastructure components used for orienting buried pipelines [1] along their route (Fig. 1). In addition, these components are also used in a wide range of applications, including critical piping of storage tanks [2], power plants [3], industrial facilities [4], and even offshore platforms [5-6]. When these critical components are subjected to extreme events such as fault ruptures, lands, and repeated loadings, the pipeline network becomes highly vulnerable, resulting in service disruptions and economic losses. In addition to the failures of the pipelines, loss of containment of these storage tanks, power plants, and

industrial facilities can be experienced due to the uplift effect under repeated loads at tank surfaces, tee connections, and nozzles. It can be hazardous to the environment and human health.

Due to the complexity of these pipeline networks, the stresses and deformations these systems undergo might be quite different from the conventional straight pipes due to their flexible characteristics. In case of severe loading conditions, cross-sectional ovalization and ratcheting failures govern the bending capacity and failure modes that are directly associated with the ratio of  $(D/t)$  and  $(R/D)$  where the pipe diameter is  $D$ , the wall thickness is  $t$ , and the radius of elbow curvature is  $R$ .

\*Corresponding author.

\*E-mail address: [ercan.kaya@alanya.edu.tr](mailto:ercan.kaya@alanya.edu.tr)





**Figure 1.** (a) pipe elbow [7] used for; (b) routing of natural gas pipeline [8].

In the literature, most of the studies on pipe elbows are focused on variational  $D/t$  and  $R/D$  ratios. Much research [9–13] focused on  $D/t$  ratios ranging from 10 to 97. Among these studies, Sobel and Newman [9] tested a  $90^\circ$  seamless pipe elbow and verified the results using the finite element method considering large displacements and material nonlinearity. Suzuki and Nasu [10] studied a welded  $90^\circ$  elbow component under in-plane bending loads. Another research study [11] employed a  $90^\circ$  pipe elbow with a bending curvature-to-diameter ratio of  $R/D = 3$ . A comprehensive research study [12] elaborated on the mechanical behavior of  $90^\circ$  pipe elbows focused on failure modes depending on the effects of  $D/t$  ratio and internal pressure levels. The studies are lately evolved into promoting material sustainability and life estimation for pipe elbows [13] to increase the fatigue life of pipe elbows.

Most of these studies address toe pipe elbows when used for industrial piping systems with relatively small pipe diameters. As for the large-diameter buried steel pipelines,  $D/t$  and  $R/D$  ratios are expected to be higher due to the practicing devices for cleaning, inspection, dimensioning, and testing purposes [14]. In literature, the diameters of pipe elbows, which have been studied experimentally and numerically for the transmitting pipeline systems, remained limited in a range of 100 [15] to 400 mm [16] for a  $90^\circ$  elbow pipe.

Oil, gas, and especially water transmission pipelines are made of large-diameter steel pipes starting from 450 mm up to 2540 mm due to the high amounts of products to be transported. In this study, the geometrical parameters of a well-documented steel water transmission line [17–20] with a diameter of 2200 mm are chosen to reveal the mechanical behavior of large-diameter steel pipe elbows under cyclic loading. The main parameters to be investigated within this research study are the elbow angles ( $90^\circ$ ,  $60^\circ$ , and  $30^\circ$ ) and internal pressure,  $p_i$ , as per operating conditions reported in related documents [17]. The bending curvature-to-diameter ratio,  $R/D$ , is chosen as five, which is the mode that

allows proper pigging operations for the buried pipelines in practical applications.

Preliminary calibration studies are conducted based on a given experimental research study [4], as detailed in the following section. Geometrical and material assumptions are made in accorded reference. After verification studies, the results of the numerical studies are explained.

## 2. NUMERICAL SIMULATION

### 2.1. Finite Element Modeling

This study uses a finite element (FE) model by software. Geometrical and material nonlinearities are taken into unconsidered predicting the post-buckling behavior and the failure modes. For this purpose, calibration studies were performed before this on previous experimental and numerical research work [4]. A 203 mm long SCH40 pipe elbow with a diameter of  $D = 219.1$  mm and a wall thickness of  $t = 8.18$  mm was tested under cyclic loading with an elbow curvature radius of  $R = 305$  mm. Steel pipe material was employed as P355N following EN 10216-3 code corresponding to ANSI/API 5L X52 steel grade. The FE model consists of two straight parts with a length of  $5D$  connected to the pipe elbow by tie connection (Fig. 2). Both pipe elbow and straight parts are C3D8R solid elements with equal wall thickness. A kinematic coupling algorithm specifies boundary conditions at the center

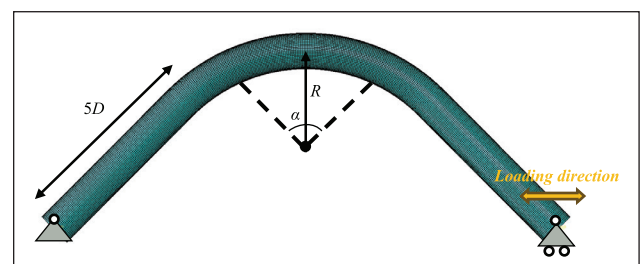


**Figure 2.** The radius of pipe curvature,  $R$ , and boundary conditions of a  $90^\circ$  elbow.

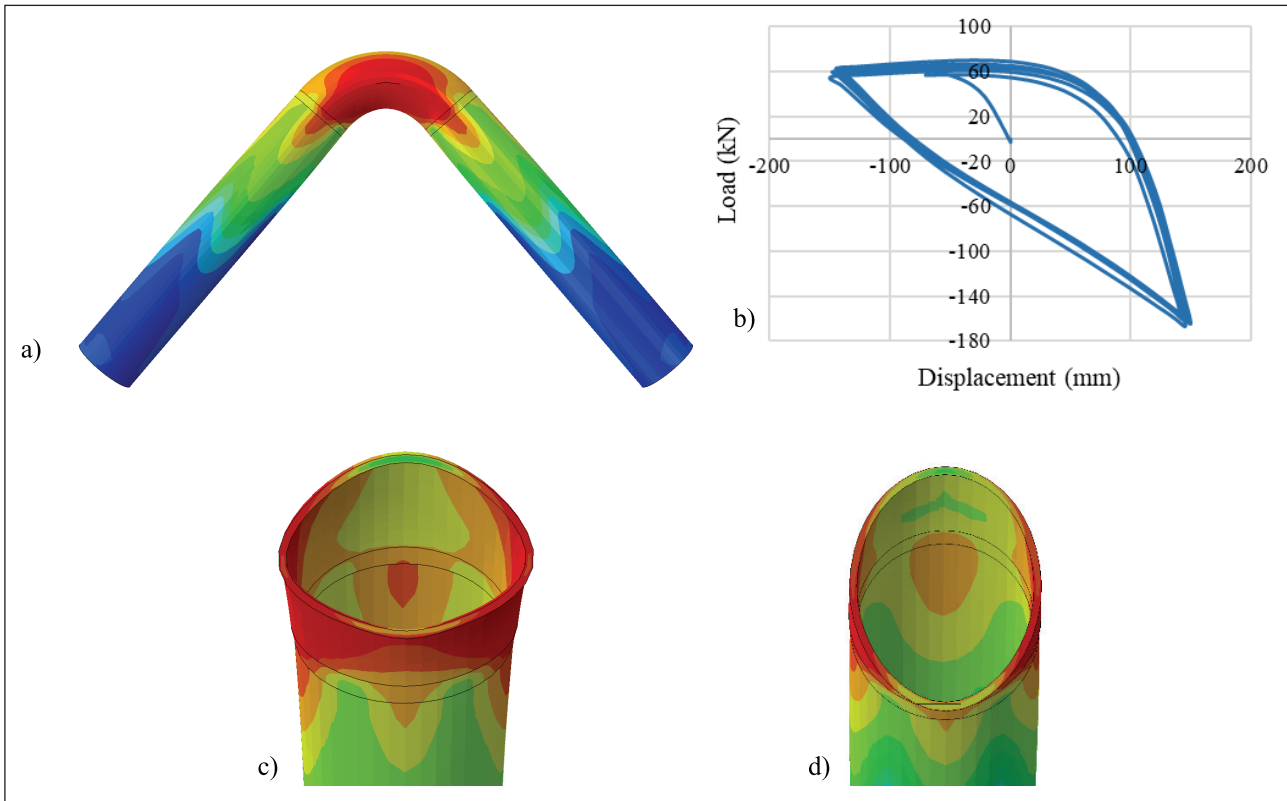


**Figure 3.** (a) pipe deflection at elbow crown due to material plasticity (b) hysteresis curve (c) closing and (d) opening ovalization.

of straight pipe ends with pinned and roller supports. A displacement boundary condition is defined on the right side as roller support (in-plane) with a cyclic loading protocol of 1.0 to 3.0 meters. For this purpose, numerical analyses were conducted using a low-cyclic loading procedure under a general static step after applying internal pressure.

The results were obtained for the pipe elbow under 3.2 MPa operating pressure with  $\pm 150$  mm of loading amplitude. The model captured the similar ratcheting behavior of the pipe elbow when a combined isotropic/kinematic hardening model was employed. The pipe deflection (Fig. 3.a) was formed due to accumulated stresses at the elbow crown after 61 cycles. The hysteresis curve (Fig. 3.b) was obtained at the released end of the pipe constraint and verified with the related research work about material nonlinearity. The von-mises stress contours depict the yielded area, including failure of the pipe elbow due to repeated closing (Fig. 3.c) and opening (Fig. 3.d) forms under cyclic loading.

As for the mechanical behavior of a large-diameter water pipeline, Kullar water steel pipeline ( $D = 2200$  mm) properties were investigated under three different cases of elbow angle,  $\alpha$  such as  $90^\circ$ ,  $60^\circ$ , and  $30^\circ$ . The steel grade utilized in this research study was chosen API 5L Grade B steel grade by the properties of the actual water pipeline [17]. Besides, the internal pressure  $p_y$  was taken at 1.0

MPa, corresponding to the operating pressure specified in the reference. The  $R/D$  ratio is also chosen as 5 for the buried pipelines that allow proper pigging operations [14], whereas the pipe has an 18 mm thickness ( $D/t = 122$ ).

## 2.2. Material Model

An inelastic material property, Armstrong-Frederic (AF) nonlinear kinematic hardening model, is defined through the ABAQUS material library that allows to capture Bauschinger effect and accumulated plastic strain (ratcheting effect) for metals subjected to cyclic loading [21]. The combined isotropic/kinematic hardening algorithm introduces the concept of change in the center of yield surface for the metals under cyclic loading, allowing the main difference between yield and back stresses. The kinematic hardening component is given as:

$$\dot{\alpha} = C\dot{\epsilon}^p - \gamma\alpha\dot{\epsilon}_q \quad (1)$$

Where  $C$  stands for kinematic hardening modulus,  $\gamma$  is the decreasing rate due to increasing plastic strain,  $\dot{\epsilon}^p$  And  $\alpha$  is back stress. In addition, the equivalent plastic strain  $\dot{\epsilon}_q$  It also is defined as:

$$\dot{\epsilon}_q = \sqrt{\frac{3}{2}\dot{\epsilon}^p : \dot{\epsilon}^p} \quad (2)$$

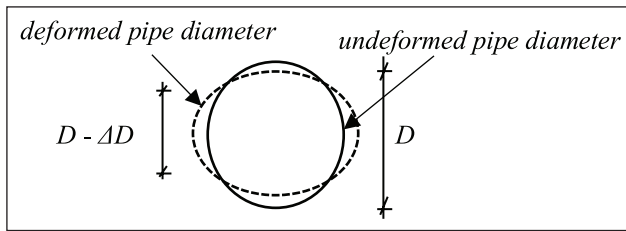


Figure 4. Cross-sectional distortion-based ovalization.

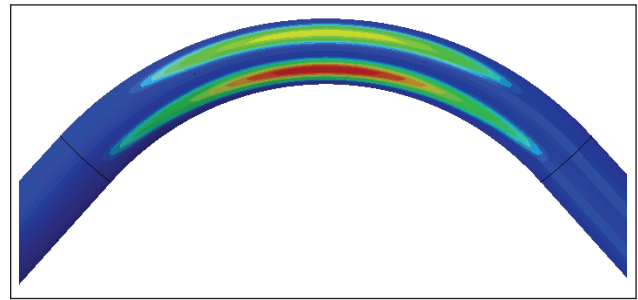


Figure 6. Plastic zone formation of 90° pipe elbow under 1.0-meter cyclic loading.

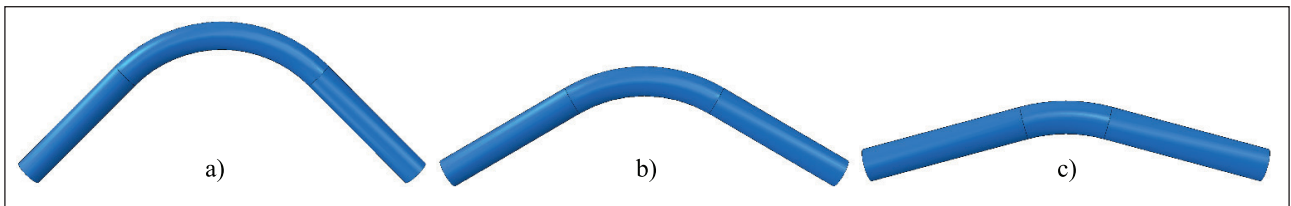


Figure 5. a) 90°, b) 60° and c) 30° pipe elbows.

Due to the lack of experimental data, the mechanical properties of the water pipe are taken by the API 5L Grade B with a modulus of elasticity,  $E = 221.37$  GPa, yield stress of  $\sigma_y = 293.27$  MPa, and ultimate tensile strength of  $\sigma_u = 480.13$  MPa as given in the reference study [22]. The relevant stress-strain curve is also integrated into the combined isotropic/kinematic hardening model using data type aa s half cycle.

### 2.3. Performance Criteria of Steel Pipes

According to the American Lifeline Alliance (ALA) guideline [23] tensile strain limit is 4% to maintain n pressure integrity of the pipe. Besides, the Pipeline Research Council International (PRCI) guideline [24] suggests limiting tensile strain to 2-4% for pressure integrity and 1-2% for normal operability. On the other hand, the compressive strain limit state, which corresponds to the pressure loss, is reached when the plastic strain rate is equal to  $1.76 t/D$  in both guidelines. Moreover, Gresnigt [25] suggested a flattening parameter,  $f$ , to clearly describe cross-sectional distortions as an ovalization limit state which is:

$$f = \Delta D/D \quad (3)$$

And it is assumed that the cross-sectional limit state is reached when the flattening parameter equals 0.15 (Fig. 4).

## 3. NUMERICAL RESULTS

The mechanical behavior of steel pipe elbows is investigated for three different elbow angles, as given in Fig. 5. The hysteresis curves are obtained for each pipe elbow for the case of both pressurized and unpressurized under different ranges of lateral cyclic movements. And the results

are discussed in terms of the performance mentioned above criteria and limit states.

### 3.1. 90° Pipe Elbow

For two cases, 1.0, 2.0, and 3.0 meters of cyclic loading protocol are subjected to the 90° pipe elbow. As for the pressurized pipe elbow, it is seen that the compressive strain limit state was reached after 32 cycles with a plastic strain value of 1.46% under 1.0 meters of lateral cyclic loading. When the pipe undergoes cyclic loading without having internal pressure, the pipe distortion and ovalization become more critical, and the limit state is reached due to the flattening parameter. However, there was no buckling formation for 2.0 and 3.0 meters of cyclic loading for 90° pipe elbows. The plastic formation zone was observed close to the elbow crown, especially on the intrados side of the pipe elbow (Fig. 6).

Besides, the limit plastic strain levels were reached under fewer cycles as the lateral displacement range increased. The hysteresis curves are given in Fig. 7 for both pressurized and unpressurized cases under 1.0, 2.0, and 3.0 meters of cyclic loading.

### 3.2. 60° Pipe Elbow

According to the numerical result of the 60° pipe elbow, the limit plastic strain levels are reached at earlier stages (fewer cycles) compared to the 90° pipe elbow. It is seen that the plastic zone is shifted from the elbow flank to intrados under 1.0 meters of cyclic loading (Fig. 8). Moreover, the more the pipe elbow angle decreases, the more the pipe system becomes vulnerable to kink or buckling effect under same repeated displacements. The hysteresis curves obtained for 60° pipe elbow are given in Fig. 9 below. The tensile strain limit state is reached at the 4<sup>th</sup> cycle with a

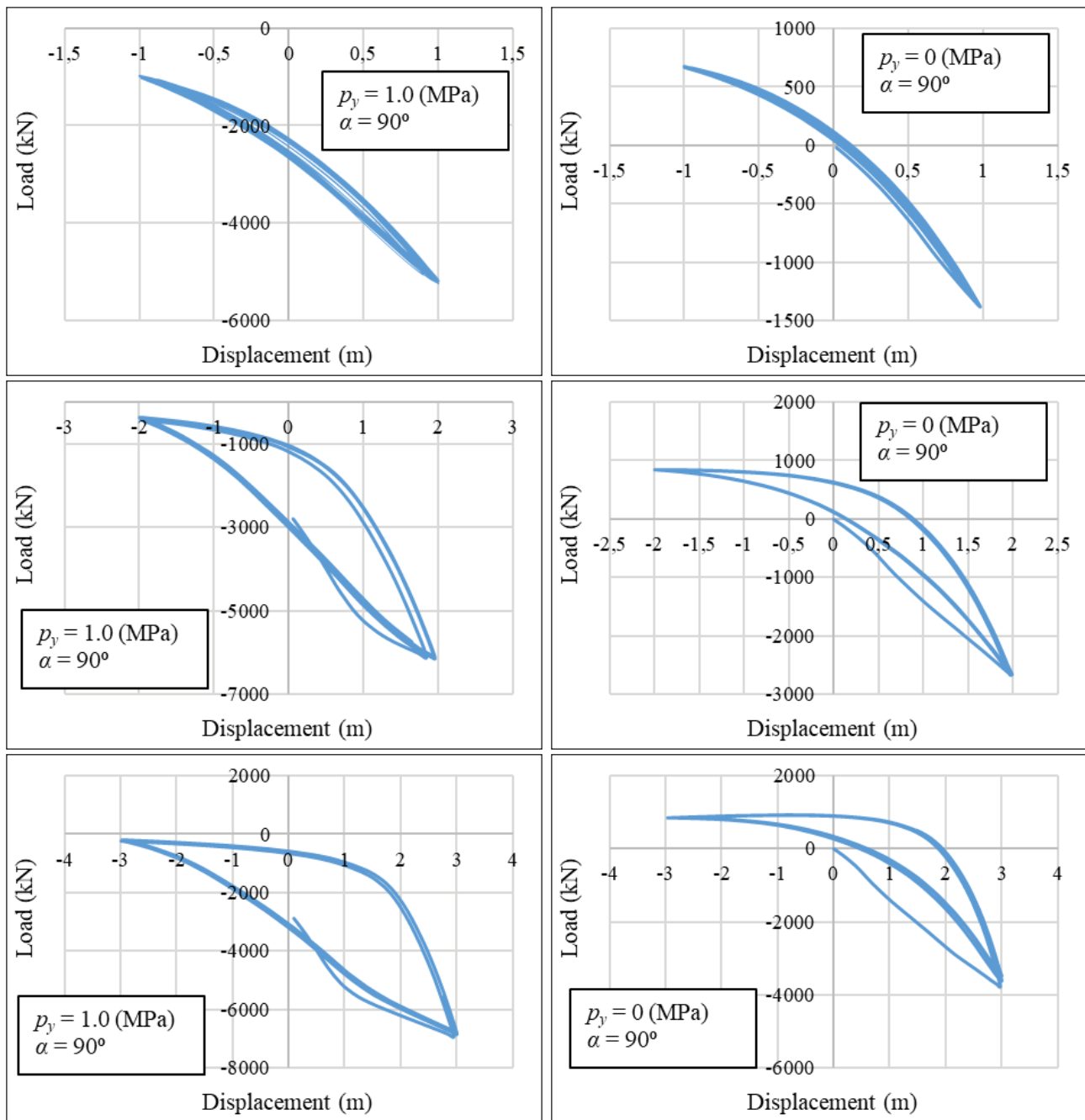


Figure 7. Hysteresis curves for 90° pipe elbow.

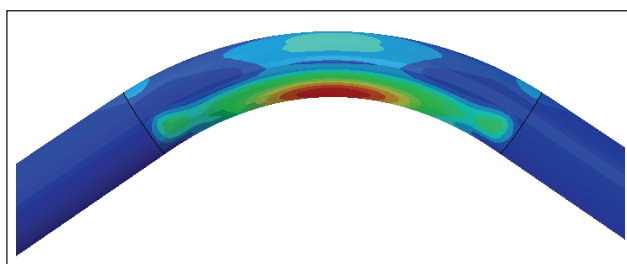


Figure 8. Plastic zone formation of 60° pipe elbow under 1.0-meter cyclic loading.

plastic strain value of 1.63%, and the flattening ratio is exceeded the critical value of 0.15. Similar to the 90° pipe elbow, the formation of plastic deformation is delayed under operating pressure. However, there was no sight of buckling formation under 1.0 and 2.0 meters of cyclic loading but only under 3.0 meters of repeated loads.

### 3.3. 30° Pipe Elbow

As for the 30° pipe elbow, the pipe’s flexibility has remarkably reduced due to a decrease in the elbow angle, and yield strains were reached at the beginning of the

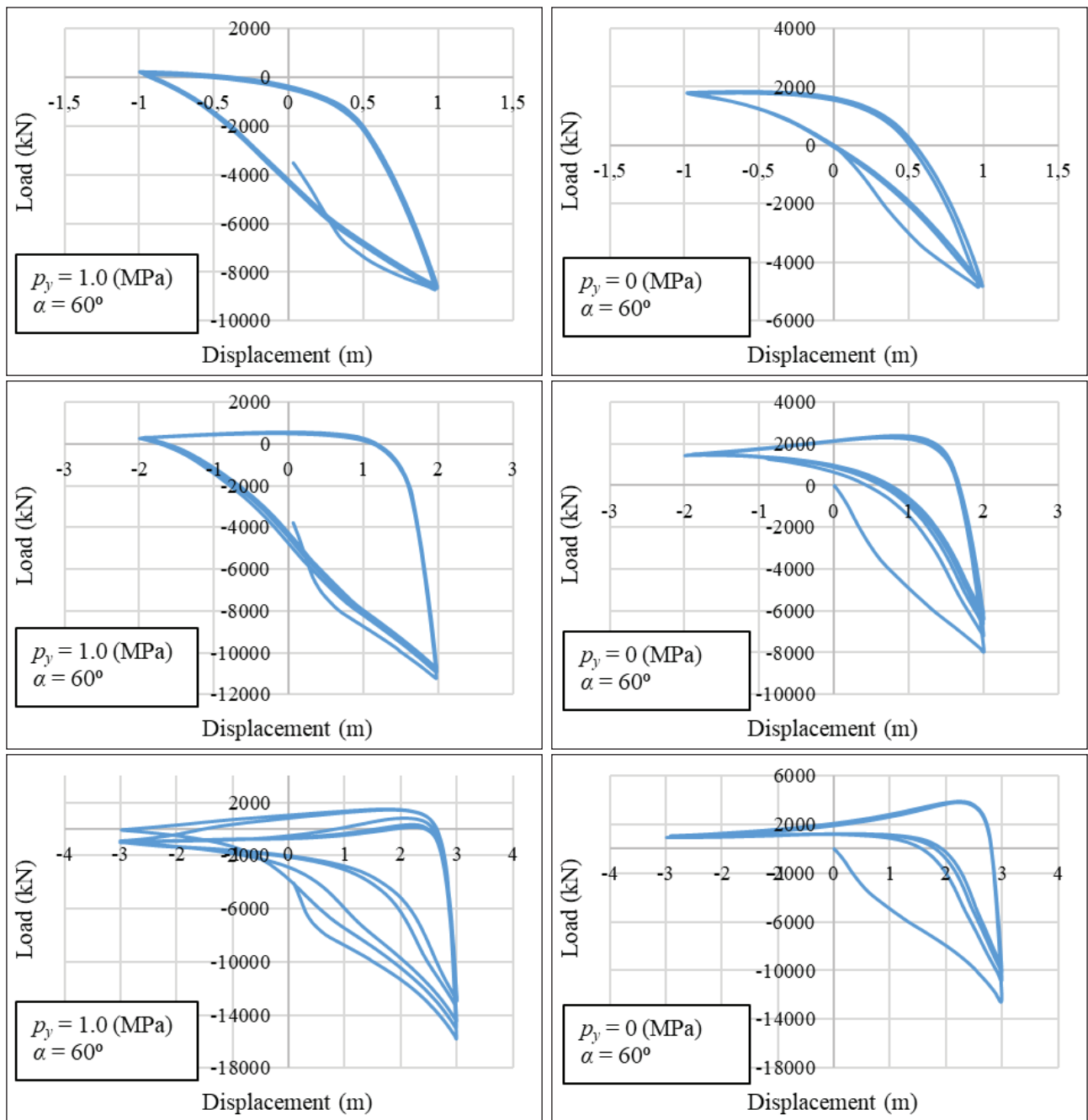


Figure 9. Hysteresis curves for 60° pipe elbow.

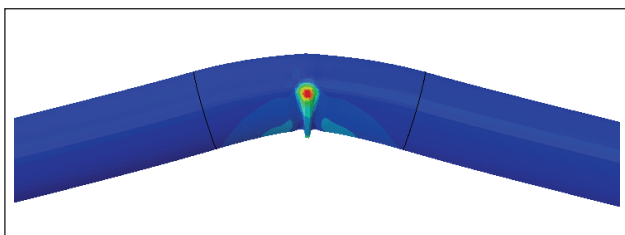
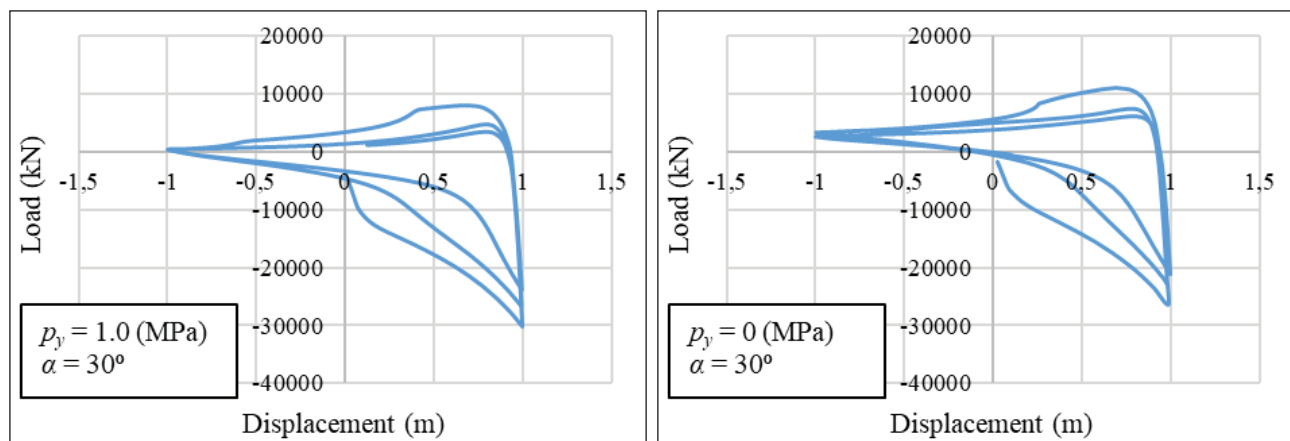


Figure 10. Plastic zone of 30° pipe elbow under 1.0-meter cyclic loading.

loading protocol. It is seen that the pipe elbow behaves similarly to the straight pipes, where tensile and compression limit states are mainly governed. Due to high plastic strain values, only 1.0 meter of cyclic loading results were obtained for the 30° pipe elbow, where the buckling formation was observed as in Fig. 10. Also, the decrease in the number of cycles before the plastic strains were observed in Fig. 11.



**Figure 11.** Hysteresis curves for 30° pipe elbow under 1.0 meters of cyclic loading.

The numerical results have verified the relation between pipe elbow angle and flexibility which might become critical in providing the structural integrity of pipeline systems. It should be noted that the pipe elbows behave similarly to the straight pipes as the elbow angle decreases and become more vulnerable to plastic deformations. Moreover, the fatigue life of pipe elbows with a higher angle expands due to their higher tolerance for repeated loads before reaching limit state values.

The findings of this study can be applied to pipelines, pipe-tank connections and industrial facilities, power plants, and many other practical scenarios. However, the surrounding soil effect for buried pipelines should also be considered in predicting local strains, which might easily be affected by soil conditions (stiff and soft soil) and seismic hazard regions. Therefore, further study recommendations are provided in the conclusion section.

#### 4. CONCLUSION

Steel pipe elbows are critical infrastructure components for orienting pipelines along their routes. Promoting these systems' fatigue life and material sustainability is important, which may result in large-scale economic losses and service disruptions due to seismically induced cyclic loadings. This study investigates the mechanical behavior of large-diameter steel pipe elbows, which behaves differently from conventional straight pipes due to the stresses and deformations they undergo based on their flexible characteristics. For this purpose, a 3D nonlinear finite element model is employed and calibrated before the numerical studies. Geometrical and material nonlinearities are considered for the numerical models by adopting the Armstrong-Frederick plasticity model. Three types of pipe elbow, such as 90°, 60°, and 30°, are subjected to 1.0, 2.0, and 3.0 meters of low-cyclic loading protocol for pressed and unpressurized cases.

The results revealed that the pipes with a larger elbow angle could undergo a ignores before reaching their limit states. In addition, steel pipe elbows with small angles behave similarly to straight pipes (with less flexibility under

opening and closing bending loads) in terms of mechanical behavior, as tensile and compression limit states are mainly governed. Moreover, the vulnerability to plastic deformations, such as the formation of kink and buckling deformations, is increased compared to pipe elbows with larger angles. Unpressurized pipe elbows were also found more vulnerable to pipe distortion and ovalization.

As for further studies, the mechanical behavior of steel pipe elbows can be elaborated on the surrounding soil conditions by adopting soil-pipe interaction or equivalent soil springs for different types of soil (stiff and soft soil) and  $D/t$  ratios. Considering the distance between the fault line and pipelines supported with elbow components, local strain values, and pull-out forces can be elaborated. In addition, innovative and advanced materials, including geometrically improved flexible joints, can improve the seismic performance of steel pipe elbows under severe ground motions.

#### ETHICS

There are no ethical issues with the publication of this manuscript.

#### DATA AVAILABILITY STATEMENT

All graphs and data obtained or generated during the investigation appear in the published article.

#### CONFLICT OF INTEREST

The authors declared no potential conflicts of interest with respect to the research, authorship, and/or publication of this article.

#### FINANCIAL DISCLOSURE

The author declared that this research study has received no financial support.

#### AUTHOR'S CONTRIBUTIONS

The author confirms sole responsibility and contribution for the study conception and design, analysis and

interpretation of results, and manuscript preparation. Further, the author has validated and approved the final manuscript.

### PEER-REVIEW

Externally peer-reviewed.

### REFERENCES

- [1] Vazouras, P., & Karamanos, S. A. (2017). Structural behavior of buried pipe bends and their effect on pipeline response in fault crossing areas. *Bulletin of Earthquake Engineering*, 15, 4999-5024. [CrossRef]
- [2] Vathi, M., Karamanos, S. A., Kapogiannis, I. A., & Spiliopoulos, K. V. (2017). Performance criteria for liquid storage tanks and piping systems subjected to seismic loading. *Journal of pressure vessel technology*, 139(5), 051801. [CrossRef]
- [3] Kim, S. W., Jeon, B. G., Hahm, D. G., & Kim, M. K. (2023). Failure criteria evaluation of steel pipe elbows in nuclear power plant piping systems using cumulative damage models. *Thin-Walled Structures*, 182, 110250. [CrossRef]
- [4] Varelis, G. E., Karamanos, S. A., & Gresnigt, A. M. (2013). Pipe elbows under strong cyclic loading. *Journal of Pressure Vessel Technology*, 135(1), 011207. [CrossRef]
- [5] Daliri, A. K., & Naimi, S. (2016). Dynamic analysis of fixed marine risers with 1st and 5th order Rogue Waves. *Journal of Engineering Research*, 4(3), 43-56.
- [6] Daliri, A. K., & Naimi, S. (2018). Transient dynamic analysis of the high-specific-strength steel jacket with extreme wave and vessel impact load. *Acta Scientiarum. Technology*, 40. [CrossRef]
- [7] Futura Sciences. (2023). *Sustainable development. Gas pipeline*. <http://www.futura-sciences.us/dico/d/sustainable-development-gas-pipeline-50000943/>
- [8] Hydrocarbons Technology. *Midship Natural Gas Pipeline*. (2023). <https://www.hydrocarbons-technology.com/projects/midship-natural-gas-pipeline-oklahoma-usa/>
- [9] Sobel, L. H., & Newman, S. Z. (1980). Comparison of experimental and simplified analytical results for the in-plane plastic bending and buckling of an elbow. *J Pressure Vessel Technology*, 102, 400-409. [CrossRef]
- [10] Suzuki, N., & Nasu, M. (1989). Non-linear analysis of welded elbows subjected to in-plane bending. *Computers & Structures*, 32(3-4), 871-881. [CrossRef]
- [11] Chattopadhyay, J., Nathani, D. K., Dutta, B. K., & Kushwaha, H. S. (2000). Closed-form collapse moment equations of elbows under combined internal pressure and in-plane bending moment. *J. Pressure Vessel Technol.*, 122(4), 431-436. [CrossRef]
- [12] Karamanos, S. A., Tsouvalas, D., & Gresnigt, A. M. (2006). Ultimate bending capacity and buckling of pressurized 90 deg steel elbows. *Journal of Pressure Vessel Technology*, 138(4), 041203. [CrossRef]
- [13] Takahashi, K., Tsunoi, S., Hara, T., Ueno, T., Mikami, A., Takada, H., & Shiratori, M. (2010). Experimental study of low-cycle fatigue of pipe elbows with local wall thinning and life estimation using finite element analysis. *International Journal of Pressure Vessels and Piping*, 87(5), 211-219. [CrossRef]
- [14] Karamanos, S. A. (2016). Mechanical behavior of steel pipe bends an overview. *Journal of Pressure Vessel Technology*, 138(4), 041203. [CrossRef]
- [15] Yoshizaki, K., O'Rourke, T. D., & Hamada, M. (2003). Large scale experiments of buried steel pipelines with elbows subjected to permanent ground deformation. *Structural Engineering/Earthquake Engineering*, 20(1), 1-11. [CrossRef]
- [16] Cheong, T. P., Soga, K., & Robert, D. J. (2011). 3D FE analyses of buried pipeline with elbows subjected to lateral loading. *Journal of Geotechnical and Geoenvironmental Engineering*, 137(10), 939-948. [CrossRef]
- [17] Kaya, E. S., Uçkan, E., O'Rourke, M. J., Karamanos, S. A., Akbas, B., Cakir, F., & Cheng, Y. (2017). Failure analysis of a welded steel pipe at Kullar fault crossing. *Engineering Failure Analysis*, 71, 43-62. [CrossRef]
- [18] Kaya, E. Ş. (2023). Eksenel basınç kuvveti ve eğilme momentine maruz çelik boruların performans kriterlerinin saptanması. *Gazi Üniversitesi Mühendislik Mimarlık Fakültesi Dergisi*, 38(4), 2107-2118. [CrossRef]
- [19] Uçkan, E., Akbas, B., Kaya, E.S., Cakir, F., Cengiz, I., Makaraci, M., & Ataoglu, S. (2016). Design issues of buried pipelines at permanent ground deformation zones. *Disaster Science and Engineering*, 2(2), 53-58.
- [20] Kaya, E. S., Uçkan, E., Cakir, F., & Akbas, B. (2016). A 3D nonlinear numerical analysis of buried steel pipes at strike-slip fault crossings. *Grđevinar*, 68(10), 815-823.
- [21] Simulia. (2014). ABAQUS Theory Manual, Version 6.14, Dassault Systèmes.
- [22] Lim, K. S., Azraai, S. N. A., Yahaya, N., Noor, N. M., Zardasti, L., & Kim, J. H. J. (2019). Behaviour of steel pipelines with composite repairs analysed using experimental and numerical approaches. *Thin-Walled Structures*, 139, 321-333. [CrossRef]
- [23] ALA. (2005). American Lifelines Alliance Guidelines for the Design of Buried Steel Pipe. <https://www.americanlifelinesalliance.com/pdf/Update061305.pdf>.
- [24] D.G. Honegger, & D.J. Nyman. (2004). Guidelines for the seismic design and assessment of natural gas and liquid hydrocarbon pipelines, prepared for the Pipeline Design Construction & Operations Technical Committee of Pipeline Research Council International, Inc., Catalog No. L51927. [CrossRef]
- [25] Gresnigt, A.M. (1986). Plastic design of buried steel pipelines in settlement areas, *HERON*, 31(4), 1-113.